physica status solidi rrl

www.pss-rapid.com

Kinetic Study of the Thermal Quenching of the Ultraviolet Emission in Zn_2GeO_4 Microrods

Jaime Dolado, Pedro Hidalgo, and Bianchi Méndez*

Zn_2GeO_4 microrods obtained by thermal evaporation of a compacted powder mixture of ZnO and Ge exhibit quite intense UV luminescence at low temperatures. Herein, the luminescence properties of Zn_2GeO_4 microrods are studied for 2:1 and 1:1 ZnO:Ge ratio in the precursor mixture. In both cases, Zn_2GeO_4 microrods of high crystal quality produce a 355 nm emission under aforementioned bandgap excitation conditions at low temperatures. However, this emission vanishes at room temperature (RT) in the 1:1 samples while it is kept in the 2:1 ones. Herein this work, the thermal quenching of the UV luminescence is studied by means of steady and time-resolved photoluminescence techniques from 4 K up to RT for both Zn_2GeO_4 microrods. The analysis of the results leads us to conclude that although the luminescence mechanisms are the same in both cases, a higher decay rate is observed in the 1:1 in both intensity and lifetime, which explain the observed thermal quenching at RT.

1. Introduction

Zinc germanate oxide, Zn_2GeO_4, has recently emerged as an attractive white light emitter, with improved optical and electrical properties over ZnO or other related wide bandgap semiconductors.[1–3] In particular, broad visible emission bands have been reported in Zn_2GeO_4 micro- and nanomaterials with several morphologies, such as microrods, nanowires, or nanoparticles, and attributed to recombinations between oxygen vacancies (V_O)- and cation vacancies (V_{Ge}, V_{Zn})-related electronic states in the material.[4,5] Zn_2GeO_4 has also proposed as active material in solar-blind photodectectors due to its huge bandgap ($E_g = 4.6$ eV at room temperature [RT]).[6,7] In principle, the wide bandgap would also allow for ultraviolet (UV) luminescence; however, the UV emission has been scarcely reported in the literature.[5] One of the reasons could be that most of works make use of a 325 nm (3.8 eV) laser, whose photon energy lies below the Zn_2GeO_4 bandgap. Hence, high-energy photons in the UV-C range, electrons, or X-ray could be suitable excitation sources for UV emission. Recently, the electronic states in defect-free and defective Zn_2GeO_4 (O, Ge and Zn vacancies, and zinc interstitials) have been calculated via the density-functional theory (DFT) method.[8] The results show that V_O defects generate electronic states forming a broad donor level (0.3 eV width) very close to the conduction band (4.2 eV from the valence band) while zinc interstitials (Zn_i) lead to a narrow donor level at 3 eV above the valence band (VB). These energy levels could provide UV luminescence in Zn_2GeO_4.

In contrast, the influence of growth conditions on the equilibrium defect concentration and samples architecture has been appeared to play a critical role in the luminescence properties of Zn_2GeO_4.[4,9–12] Thermal annealing of precursor materials containing Zn and Ge has been revealed as an effective method to produce high-quality crystalline Zn_2GeO_4 microrods and nanowires under the vapor–solid mechanism.[5,13] In particular, luminescence in the UV and in the visible range depending on the probe energy, above of below the energy bandgap, has been observed in Zn_2GeO_4 microrods synthetized by a thermal treatment of a mixture of ZnO and Ge.[8] One of the key parameters in this case is the ratio between the precursors in the initial mixture. Actually, two UV photoluminescence (PL) bands have been reported in Zn_2GeO_4 microrods obtained by a thermal annealing of a ZnO:Ge:C mixture with a 2:1:2 ratio, attributed to the electrons recombination from V_O and Zn_i defect levels to VB holes, respectively, under aforementioned bandgap excitation conditions.[5,8]

In this work, the UV luminescence bands in Zn_2GeO_4 microrods obtained from ZnO:Ge and ZnO:Ge:C precursor mixtures in a 1:1 and 2:1:2 weight ratio, respectively, are studied by means of the temperature dependence study of the steady and time-resolved photoluminescence (TR-PL) spectra. A higher concentration of ZnO in the initial mixture leads to UV luminescence up to RT, while the other one exhibits a thermal quenching of the UV emission. The kinetics of the UV luminescence band as a function of temperature is discussed in terms of the non-radiative channels that can be deduced from the Arrhenius plot of the PL intensity and lifetime decay in both cases.

J. Dolado, P. Hidalgo, B. Méndez
Department of Materials Physics
Faculty of Physical Sciences
University Complutense of Madrid
E-28040 Madrid, Spain
E-mail: jdolado@ucm.es

The ORCID identification number(s) for the author(s) of this article can be found under https://doi.org/10.1002/pssr.202100613.

DOI: 10.1002/pssr.202100613

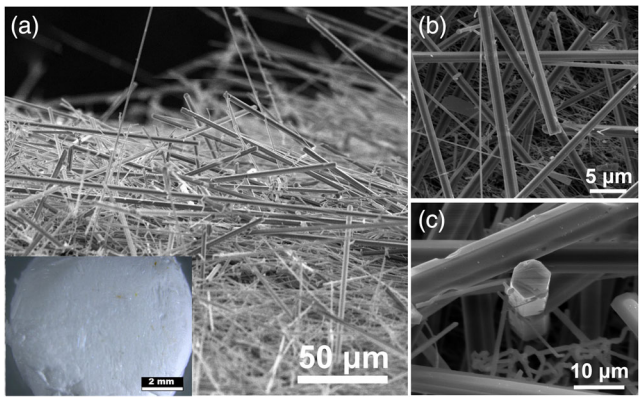

Figure 1. a) Scanning electron microscope (SEM) image of a general view of the Zn_2GeO_4 microrods studied in this work. The inset shows the optical image of the pellet fully covered by a white coating of structures. SEM images of b) several Zn_2GeO_4 microrods and c) a detailed view of a microrod showing the hexagonal shape.

2. Thermal Quenching in Zn_2GeO_4 Microrods

2.1. Zn_2GeO_4 Microrods: Different Precursor Ratio

ZnO:Ge (1:1) precursors produces a huge white mat of structures after the dynamic thermal annealing that fully cover the substrate, as it can be observed in the optical image and in the secondary electron (SE) image of **Figure 1**a. The thermal treatment of the T(21) pellet produces as well similar Zn_2GeO_4 microrods; however, the density of microstructures over the pellet is lower than in T(11). Figure 1b,c shows SE images with the detail of some Zn_2GeO_4 microrods, in which most of them appear to exhibit a hexagonal cross-section shape. The transverse dimensions range from 500 nm up to about 4 μm and their lengths extend up to hundreds of microns in both samples.

Figure 2 shows the results of the structural characterization of T(11) sample, where higher amount of structures are produced (the X-ray diffraction [XRD] pattern of T(21) sample has been published previously).[5] The XRD analysis show that all diffraction peaks correspond to the rhombohedral crystal structure

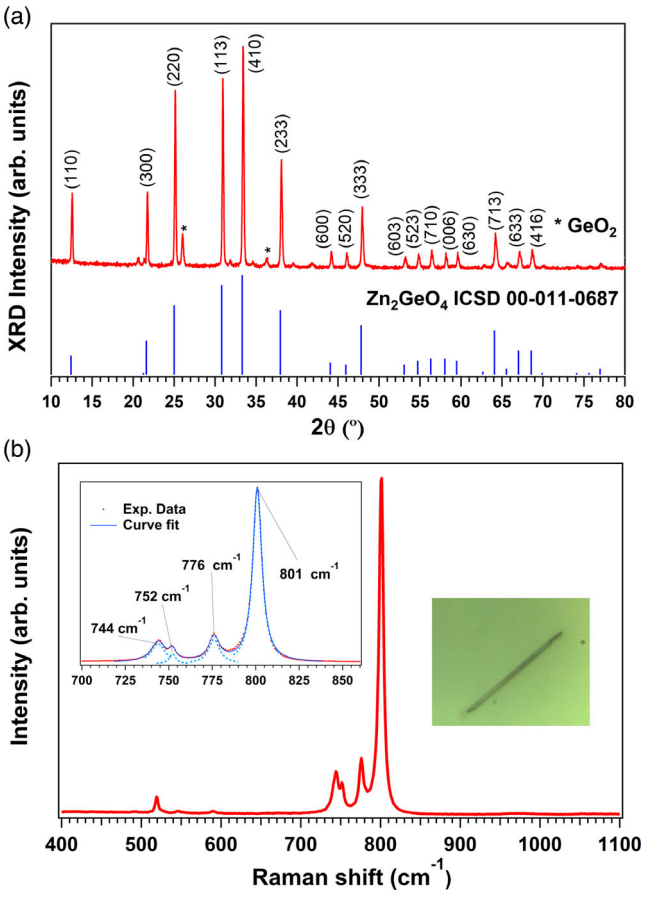

Figure 2. a) X-ray diffraction (XRD) pattern acquired on the structures obtained after the thermal treatment (red line). Peaks maxima agree with the rhombohedral structure of Zn_2GeO_4 (blue line). The * symbol indicates the peaks corresponding to the GeO_2 phase. b) Raman spectrum from a selected microrod deposited on silicon wafer.

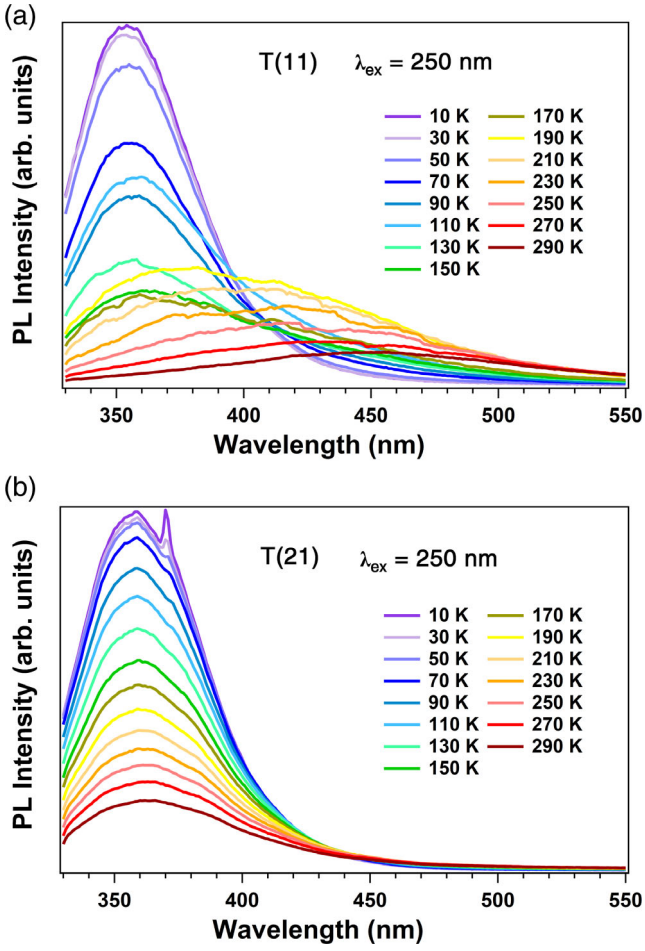

Figure 3. Photoluminescence (PL) spectra as a function of the temperature obtained under 250 nm excitation wavelength between 10 and 300 K of a) T(11) sample and b) T(21) sample.

of Zn_2GeO_4 (inorganic crystal structure database (ICSD) Collection Code: 68 382) with cell parameters $a = b = 14.28$ Å and $c = 9.54$ Å. Two weak peaks associated with some residual GeO_2 were also detected (Figure 2a). In contrast, the micro-Raman spectrum from individual microrods (Figure 2b) shows the characteristic Raman peaks of Zn_2GeO_4 at 745 ($A_g^{(1)}$), 751 ($E_g^{(3)}$), 777 ($E_g^{(4)}$), and 802 ($A_g^{(2)}$) cm^{-1}, which are associated with Ge–O–Zn symmetric and asymmetric vibration modes and the O–Ge–O bending and stretching modes, respectively.[14] All these main peaks are very well defined. The structural characterization confirms a high-quality crystalline material.

2.2. Temperature Dependence of Luminescence Intensity and Lifetimes

Figure 3a shows the series of PL spectra acquired over Zn_2GeO_4 microrods in T(11) from 10 K up to RT under excitation with a Xe lamp monochromated at 250 nm (5.1 eV), in which two broad emission bands in the UV and in the blue range are observed with noticeable changes as a function of the temperature. At low temperatures, the UV (355 nm) band is the only emission, whereas a blue band emerges at certain temperature as the temperature increases, becoming the dominant one at RT. In the case of T(21) sample, the PL emission, under the same excitation conditions, only shows a complex UV emission in the whole temperature range, as Figure 3b shows.

As it has been mentioned earlier, the origin of the UV and blue emissions may be related to electrons recombination between oxygen-vacancy (VO)-related levels, which act as donors, with VB or acceptor level holes, respectively.[4,8,12] The narrow UV peak at 380 nm, resolved at low temperatures in the T(21) sample, was attributed to the presence of Zn_i, acting as donors instead of the VO.[8]

To elucidate the quenching of UV emission in T(11) microrods at RT, TR-PL measurements have been carried out. TR-PL provides valuable information about the luminescence mechanisms in semiconductors by monitoring the PL decay after an excitation pulse, which allows to calculate the lifetime of the recombination processes. In particular, an exponential decay is expected for the UV emission that involves recombination between V_O level electrons and VB holes, in the form $I(t) = B\exp(\frac{-t}{\tau_i})$.[15] The PL decay curves of the UV (355 nm) emission at 4 K under excitation with a pulsed light-emitting diode (LED) are shown in **Figure 4**a,b for both T(11) and T(21) samples. The instrument response (IR) after stimulation is also displayed as a black line. The fitting of experimental data yielded values of $\tau = 55$ and 68 ns, for the T(11) and T(21) samples, respectively. TR-PL measurements from 4 K up to 90 K are shown in Figure 4c,d for T(11) and T(21), respectively. Above 90 K, the lifetime of the UV emission from T(11) is too short to be measured. As a first observation, a different decay behavior between samples, that will be later analyzed, is clearly noticed between both samples.

The different quenching behavior in the UV intensity and in the lifetime as a function of the precursor ratio is another proof of the critical dependence of the luminescence properties on the

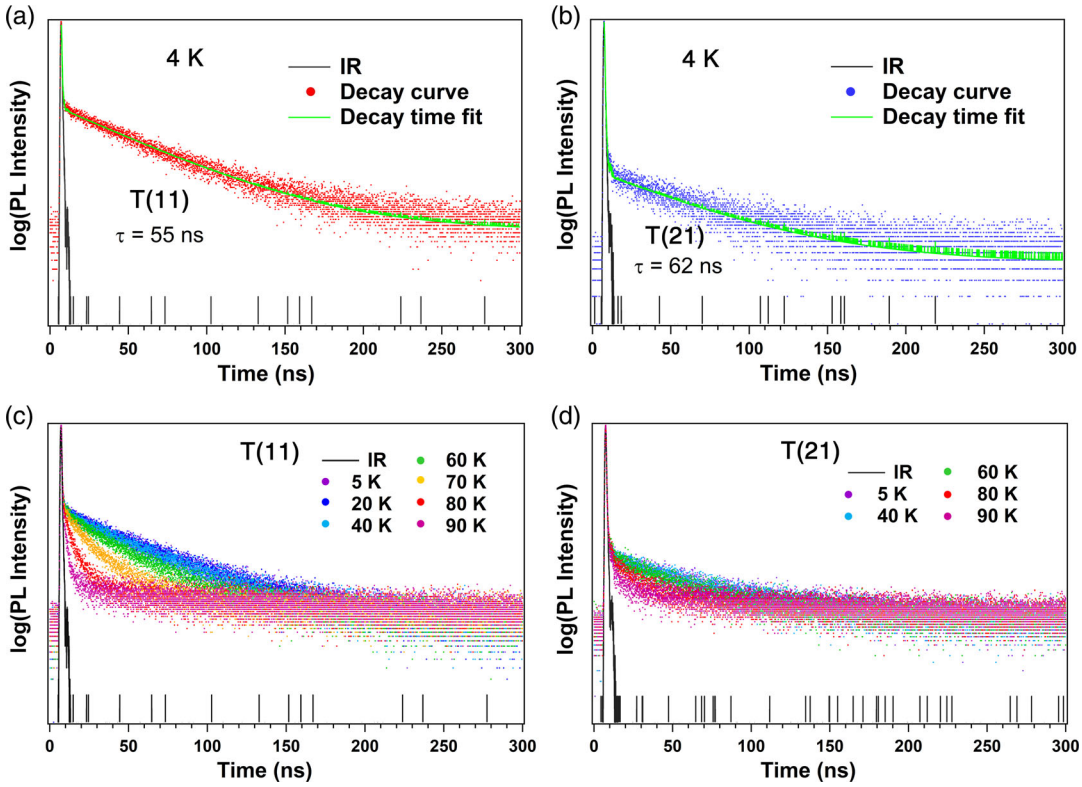

Figure 4. Decay of PL after laser pulse at different temperatures (between 5 and 90 K) for the UV band (at 355 nm) in a) T(11) and b) T(21) samples. c,d) The decay time fits (green solid lines) to the 4 K curves, which have been obtained taking into account the instrument response (black solid line).

synthesis route of the material, in this case, just by modifying the precursor ratio between Zn and Ge. Therefore, a detailed analysis of the temperature dependence of the PL intensity both under constant or pulsed illumination has been carried out to get more insight into the luminescence mechanisms in Zn_2GeO_4.

The temperature quenching of PL that involves defect-related centers in semiconductors has been explained in the framework of several models[16] that use the empirical Arrhenius expression, in which an activation energy, E_{a1}, is included.[17,18]

$$I^{PL}(T) = \frac{I_0^{PL}}{1 + A\exp(-E_{a1}/k_B T)} \quad (1)$$

where I_0^{PL} denotes the PL emission intensity in the limit of low temperatures, A is a constant, k_B is Boltzmann's constant, and E_{a1} is an activation energy. Depending on the model, this E_{a1} could be ascribed to some features occurring during the luminescence process that involve defect-related centers.

The simplest model (Seitz-Mott) refers to one defect-related center, in which its excited and ground states are described through the configuration coordinate model. In this case, the activation energy is the energy difference between the crossover of excited and ground states and the potential minimum of the excited state. Another model (Schön-Klasens [multicenter] interprets E_{a1} as the ionization energy of the eventual donor or acceptor center involved in the PL emission, and an additional non-radiative level is required for thermally emitted holes or electrons to recombine, so it is also called multicenter model. However, these models sometimes fail to explain the PL-quenching behavior when it occurs abruptly. Reshchikov et al. have proposed a third PL-quenching mechanism for high-resistivity semiconductors when the PL intensity suddenly drops at some critical temperature (T_0) as it has been reported in GaN, and in some high-resistive semiconductors.[19] In this case, even though the PL intensity is also fitted to the Arrhenius formula, the physical meaning of the activation energy is not as straightforward understood as in the former models, since additional deep defect-related levels interplay in the thermal PL quenching as temperature raises. Zn_2GeO_4 exhibits a wide bandgap, with a complex landscape of native defects that could add deep and shallow defects competing in the luminescence process. The PL quenching results in Zn_2GeO_4 show a rather sharp decay of PL intensity at certain T_0, which might favor the third proposed last approach.

Figure 5a shows the integrated PL intensity of the UV band as a function of $1/k_B T$ in the temperature range from 10 to 200 K for T(11) and T(21) samples. The sharp decay and the T_0 (marked with a dotted line) is similar in both samples, which could suggest a similar non-radiative level responsible for luminescence quenching. The fitting parameters of experimental data to Equation 1 are shown in **Table 1**.

In contrast, the PL lifetime measured in TR-PL experiments from 4 K up to 90 K can be fitted to the following expression.[20,21]

$$\tau(T) = \frac{\tau_0}{1 + C\exp(-E_{a2}/k_B T)} \quad (2)$$

where τ_0 is the PL lifetime at low temperatures when the thermal quenching of PL can be ignored ($T < T_0$), E_{a2} is the ionization energy, and C is a coefficient related to several parameters, such as the absolute internal quantum efficiency, the effective density of states in the VB, and degeneration of the defect level.[16,20] As the temperature increases from 4 to 50 K, the PL lifetime of the UV band remains unchanged in both samples, at around 55 ns for T(11) and 66 ns for T(21). At higher temperatures, the PL lifetime decreases sharply with a slope that reveals an activation energy E_{a2} in the Arrhenius plot (Figure 5b). The fitting parameters of experimental data to Equation 2 are shown in **Table 2**.

By comparing data from Tables 1 and 2, several conclusions can be drawn. First, at low temperatures, the PL intensity remains independent of the temperature, while for $T > 40$ K,

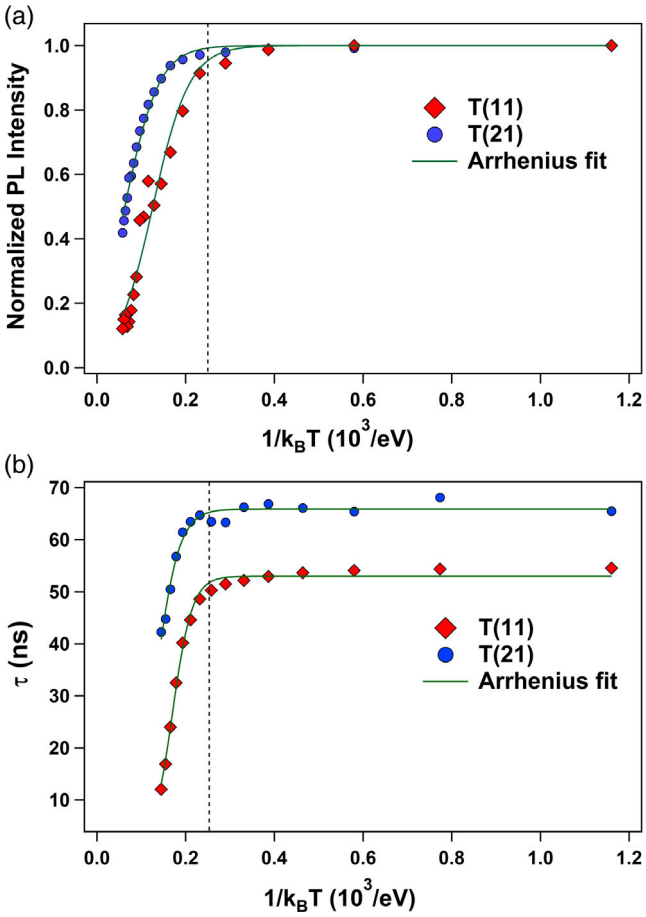

Figure 5. Temperature dependence of a) PL intensity and b) PL lifetime for the UV band in T(11) (diamonds) and T(21) (circles) samples. Experimental data are represented in comparison with a theoretical fitting (green lines) following Equations 1 and 2 (respectively). The black dashed line indicates the critical temperature T_0 from which both PL lifetime and intensity decrease more significantly.

Table 1. Fitting parameters of experimental temperature dependent photoluminescence (PL) intensity to Equation 1.

Sample	E_{a1} [meV]	A
T(11)	24	21
T(21)	26	5

Table 2. Fitting parameters of experimental temperature dependent lifetime to Equation 2.

Sample	τ_0 [ns]	E_{a2} [meV]	C
T(11)	55	42	1300
T(21)	66	37	140

the PL intensity decays exponentially. The activation energies of the non-radiative centers are found to be similar in both samples (24 and 26 meV). However, the higher quenching coefficient, *A*, in T(11) indicates a higher efficiency of the non-radiative channel in these samples. In contrast, PL lifetime temperature-dependence measurements reveal a similar trend than PL intensity. Lifetime remains constant at low temperatures and decays sharply from 40 K onward. A higher decay rate in T(11) (both in PL intensity and lifetime) compared to T(21) reveals a higher efficiency of the radiative mechanism in T(21), which explains why the UV emission is still visible at RT in this sample.

3. Conclusions

The ultrawide bandgap of Zn_2GeO_4 would allow ultraviolet emission under suitable excitation conditions; however, this emission is scarcely reported. In this work, Zn_2GeO_4 microrods obtained by thermal evaporation of a compacted powder mixture of different ZnO:Ge ratios (1:1 and 2:1) have been studied from the luminescent point of view. Both treatments have led to quite intense UV luminescence (355 nm) at low temperatures due to recombination between V_O-related levels and photo-generated holes in the VB. However, this emission vanishes at RT in the 1:1 sample, while survives in the 2:1 one up to RT. Temperature-dependent PL intensity and lifetime measurements show an abrupt PL quenching and have allowed us to evaluate the non-radiative channel in the 5–90 K temperature range in Zn_2GeO_4 microrods of both samples. The results provide similar activation energies in both cases, but a higher quenching coefficient is clearly obtained in the 1:1 sample which would explain the observed thermal quenching at RT.

4. Experimental Section

Zn_2GeO_4 microrods were synthesized by a thermal evaporation method in a tubular furnace. Two pellets of compacted ZnO:Ge and ZnO:Ge:C powders mixture with weight percentage ratios of 1:1 and 2:1:2, respectively, were prepared and thermal annealed at 800 °C under an argon flow of 1.5 l min^{-1} for 8 h. The pellets acted as source and substrate during the growth, which was based on the vapor–solid mechanism. As a result, a high amount of Zn_2GeO_4 microrods was formed on the pellet surface, with a significantly higher yield in the 1:1 pellet in comparison with the 2:1:2 one. The products were gently deposited on silicon wafer substrates to further characterization. The samples were labeled as T(11) and T(21) according to the precursor ratio of ZnO:Ge powders.

The morphological characterization was carried out in a scanning electron microscope (SEM) and structural characterization was assessed by XRD using a PANalytical X'Pert materials powder diffractometer (MPD) diffractometer and by Raman measurements in a Horiba–Jobin–Ybon confocal microscope operating with a UV 325 nm laser. Steady-state and TR-PL measurements were performed in an Edinburgh instrument FLS1000 system, equipped with double monochromator at the excitation source and a cryogenic setup to operate from 4 K up to RT. The light sources employed were a continuous 450 W ozone-free Xenon lamp for steady-state or a pulsed LED ($\lambda_{LED} = 256.8$ nm and pulses with repetition frequency of 1 MHz) for TR measurements, respectively.

Acknowledgements

This work has been supported by MINECO projects M-ERA.NET PCIN-2017-106 and MICINN project (RTI2018-097195-B-I00). We thank the CAI (UCM) for XRD facilities.

Conflict of Interest

The authors declare no conflict of interest.

Data Availability Statement

The data that support the findings of this study are available from the corresponding author upon reasonable request.

Keywords

microrods, photoluminescence, temperature dependence luminescence, thermal quenching, zinc germanate

Received: November 30, 2021
Revised: January 12, 2022
Published online:

[1] Q. Bai, P. Li, Z. Wang, S. Xu, T. Li, Z. Yang, Z. Xu, *Spectrochim. Acta A* **2018**, *199*, 179.
[2] H. He, Y. Zhang, Q. Pan, G. Wu, G. Dong, J. Qiu, *J. Mater. Chem. C* **2015**, *3*, 5419.
[3] D. Cortecchia, J. Yin, A. Petrozza, C. Soci, *J. Mater. Chem. C* **2019**, *7*, 4956.
[4] Z. Liu, X. Jing, L. Wang, *J. Electrochem. Soc.* **2007**, *154*, H500.
[5] P. Hidalgo, A. López, B. Méndez, J. Piqueras, *Acta Mater.* **2016**, *104*, 84.
[6] S. Cui, Y. Jiao, J. Liu, Y. Pu, J.-X. Wang, D. Wang, *Optik* **2021**, *235*, 166644.
[7] J. Hu, K. Liu, T. Ma, Y. Wei, J. Chen, Z. Li, *Opt. Laser Technol.* **2021**, *140*, 106946.
[8] J. Dolado, R. Martnez-Casado, P. Hidalgo, R. Gutierrez, A. Dianat, G. Cuniberti, F. Domnguez-Adame, E. Daz, B. Méndez, *Acta Mater.* **2020**, *196* 626.
[9] L. Pei, Y. Yang, L. Yang, C. Fan, C. Yuan, Q.-F. Zhang, *Solid State Commun.* **2011**, *151*, 1036.
[10] H. Tang, X. Zhu, H. He, *J. Cryst. Growth* **2016**, *451* 170.
[11] J. Dolado, P. Hidalgo, B. Méndez, *Phys. Status Solidi A* **2018**, *215*, 1800270.
[12] L. Li, Y. Su, Y. Chen, M. Gao, Q. Chen, Y. Feng, *Adv. Sci. Lett.* **2010**, *3*, 1.
[13] V.-H. Pham, V. T. Kien, P. D. Tam, P. T. Huy, *Mater. Sci. Eng. B* **2016**, *209*, 17.
[14] Y. Zhao, S. Yang, J. Zhu, G. Ji, F. Peng, *Solid State Ionics* **2015**, *274*, 12.
[15] M. Chithambo, *J. Phys. D: Appl. Phys.* **2007**, *40*, 1874.
[16] M. A. Reshchikov, *Phys. Status Solidi A* **2021**, *218*, 2000101.
[17] Z. Deng, Y. Jiang, Z. Ma, W. Wang, H. Jia, J. Zhou, H. Chen, *Sci. Rep.* **2013**, *3*, 1.

[18] M. Gerhard, B. Louis, R. Camacho, A. Merdasa, J. Li, A. Kiligaridis, A. Dobrovolsky, J. Hofkens, I. G. Scheblykin, *Nat. Commun.* **2019**, *10*, 1.
[19] M. A. Reshchikov, A. A. Kvasov, M. F. Bishop, T. McMullen, A. Usikov, V. Soukhoveev, V. A. Dmitriev, *Phys. Rev. B* **2011**, *84*, 075212.
[20] M. Reshchikov, J. McNamara, M. Toporkov, V. Avrutin, H. Morkoç, A. Usikov, H. Helava, Y. Makarov, *Sci. Rep.* **2016**, *6*, 1.
[21] M. Chithambo, *J. Phys. D: Appl. Phys.* **2007**, *40*, 1880.